

Mesoporous sol-gel deposited SiO_2 - SnO_2 nanocomposite thin films

This article has been downloaded from IOPscience. Please scroll down to see the full text article.

2012 IOP Conf. Ser.: Mater. Sci. Eng. 30 012003

(<http://iopscience.iop.org/1757-899X/30/1/012003>)

View [the table of contents for this issue](#), or go to the [journal homepage](#) for more

Download details:

IP Address: 130.209.6.41

The article was downloaded on 05/04/2012 at 14:26

Please note that [terms and conditions apply](#).

Mesoporous sol-gel deposited SiO₂-SnO₂ nanocomposite thin films

A A Ponomareva^{1,2}, V A Moshnikov¹ and G Suchanek²

¹St. Petersburg State Electrotechnical University (LETI), 197376 St. Petersburg, Russia

²TU Dresden Solid State Electronics Laboratory, 01062 Dresden, Germany

E-mail: ap_k@inbox.ru, Gunnar.Suchanek@tu-dresden.de

Abstract. Nanocomposite SiO₂-SnO₂ thin films were prepared on oxidized silicon substrates using the sol-gel technique with SnCl₂·2H₂O as a tin precursor and tetraethylorthosilicate (TEOS) as a silica source. The porous structure of the films was investigated by atomic force microscope. Gas sensitivity of the samples was measured at different temperatures and for different H₂ concentrations. Advanced gas sensing properties were obtained for a silica fraction of 10 at% providing a mesoporous microstructure.

1. Introduction

Since first proposed in 1962 [1], research efforts focused on improving the gas sensitivity of oxide semiconductor-based gas sensors. The gas detection principle of semiconductor type gas sensors is based on the variation of the depletion layer at the grain boundaries in the presence of reducing or oxidizing gases [2]. Chemisorbed oxygen species (O₂⁻, O⁻) from the air act as electron acceptors and lead to the formation of a surface depletion layer as well as a surface barrier. Upon exposure to reducing gases, their oxidation takes place at the surface resulting in lower oxygen ion coverage. This returns electrons into the SnO₂ bulk and lowering thus the surface barrier. In consequence, a decrease of the electrical conductivity is obtained.

By means of nanosized SnO₂, the operating temperature for hydrogen gas sensors can be reduced to 100-150 °C [3] compared to conventional SnO₂ sensors typically operating in the temperature range 200–500 °C [4]. SnO₂ nanostructured materials such as nanoparticles, nanorods, nanotubes, nanobelts, nanosheets, nanocubes, mesoporous structures with well aligned pores, hollow oxide structures and hierarchical nanostructures were fabricated in order to maximize gas sensing performance by increasing the surface area to volume ratio [5]. However, for SnO₂ grains with size of about 1 to 4 nm, the grain growth starts already at temperatures of 200 to 400°C. Thus, smaller grain size results in higher sensitivity, but at the same time long-term stability of gas sensors is decreased [6]. The resistance drift of SnO₂ gas sensors becomes apparent for a grain size less than 20 nm and increases up to 40% for a grain size of 2 nm during a 30-day test [3]. On the other hand, nano-sized materials easily aggregate due to their strong and inevitable van der Waals attraction which is inversely proportional to the particle size. They irreversibly tend to form hard, secondary aggregates from densely packed agglomerates of smaller grains. This hampers interdiffusion of the sensing gas toward the sensing surface as well as the counter-diffusion of the product gases to the ambient. Thus, only the primary particles near the surface region of the agglomerates contribute to the gas sensing reaction and the inner part remains inactive [6]. Moreover, the sluggish gas diffusion through the aggregated slows the gas response speed.

Recently, one of our laboratories has applied this approach for the fabrication of SnO₂-SiO₂ composites comprising hierarchical macro-, meso- and micropores (according to IUPAC notation [7]). In this work, we investigate gas sensing properties of such sol-gel deposited nanocrystalline SnO₂-SiO₂ composites in relation to their microstructure.

2. Experimental

Nanocrystalline SnO₂-SiO₂ thin films comprising a hierarchical pore structure were fabricated using a polymeric sol-gel process on oxidized silicon and quartz glass substrates. Tin(II) chloride dihydrate SnCl₂·2H₂O (M = 225.63 g/mol) was used as a tin precursor and tetraethylorthosilicate (TEOS) C₈H₂₀O₄Si (M = 208.33 g/mol) as a silica source. Solution No. 1 consisted of 10 ml (170 mmole C₂H₅OH) of 96 % ethanol as solvent, 1.07 mmole SnCl₂·2H₂O and 0.268 mmole TEOS, solution No. 2 10 ml (110 mmole) *n*-butanol as solvent, 0.683 mmole SnCl₂·2H₂O and 0.171 mmole TEOS. The solutions were aged 24 h at room temperature and spin-coated onto 3" oxidized silicon wafers and quartz glass substrates without an adhesion promoter. The films were calcined at about 550°C in air for 5 minutes by transferring the wafer into a hot furnace. Cooling down was performed in the furnace within 12 to 14 hours.

Microstructure of the deposited porous SnO₂-SiO₂ films was investigated by atomic force microscopy using an NTEGRA Thermo scanning probe microscope (NT-MDT, Zelenograd, Russia). Tapping mode imaging was performed in air using silicon cantilevers (Type NSG01, NDT-MDT, Zelenograd, Russia). The specific surface area (SSA) was measured using the Brunauer, Emmett and Teller (BET) method with nitrogen adsorption using a Sorbi-N4.1 instrument (ZAO META, Novosibirsk, Russia). The UV-VIS-NIR optical properties of the films were investigated by absolute transmission measurements in a two-beam spectrophotometer Lambda 950 (PerkinElmer, USA) in the range of 300–2000 nm with steps of 2 nm. Transmission measurements of liquid samples (sols) were performed by Lambda 900 (PerkinElmer, USA) in the same range as used for films.

Sensor structures were prepared using films deposited onto oxidized silicon substrates with *n*-butanol as a solvent. Nickel-chrome and gold layer of a thickness of 10 and 35 nm, respectively, were evaporated onto the SnO₂-SiO₂ thin films. Thereby, the Ni-Cr layer serves for adhesion improvement. The electrode layers were patterned by a copper contact mask forming 0.5 and 0.4 mm wide interdigital electrodes.

Gas sensing experiments were carried out by using nitrogen (reference gas) and 1.5 vol.% hydrogen (analyte gas) in nitrogen provided by a computer controlled gas flow system. The purity of all gases was ≥ 99.999 Vol. %. The total gas flow was kept constant at 90 sccm. A gas sensor area of about 3.5 mm² on the silicon wafer was heated using a small platinum heater. The measurement setup is described in detail elsewhere [8].

3. Results and discussion

Optical transmission spectra of sols (solutions No.1 and No. 2) were recorded before layer fabrication (figure 1(a)) and after annealing of the corresponding films (figure 1(b)). Figure 1 demonstrates that significant differences of sol-gel system optical properties were obtained only after thermal annealing. The values of absorption edge of the samples prepared using both ethanol and *n*-butanol solvents were 3.4 eV and 4.0 eV, respectively. In the *n*-butanol case the band gap is larger than the bulk value of 3.6 eV due to the contribution of quantum size effect of the present SiO₂-SnO₂ thin film [9, 10]. Moreover, the *n*-butanol solvent exhibits a higher viscosity (2.578 mPa·s at 298K [11]) compared to ethanol (1.1 mPa·s at 298K [12]). Therefore, motion and aggregation of the tin-containing clusters are slower resulting in a smaller grain size of *n*-butanol derived films.

Figure 2 shows the AFM-images of the samples. Practically no porosity was observed in films prepared without TEOS addition (fig. 2(a)). The 10 at% SiO₂-90 at% SnO₂ sample exhibits the largest porosity with a three-dimensional film structure (fig. 2(b)). The sample with 20 at% silica fraction had circular pores of different sizes (fig. 2(c)). The SSA of this film amounted to 87.21 m²/g yielding an average pore size of about 10 nm. SSA and average pore size are in good agreement with the values of similar films investigated in [13]. On the other hand, it has to be mentioned that these nanopores known to enhance gas sensitivity [14] cannot be imaged by our AFM device. A more detailed analysis of film microstructure based on fractal analysis of surface topography will be given in a forthcoming paper.

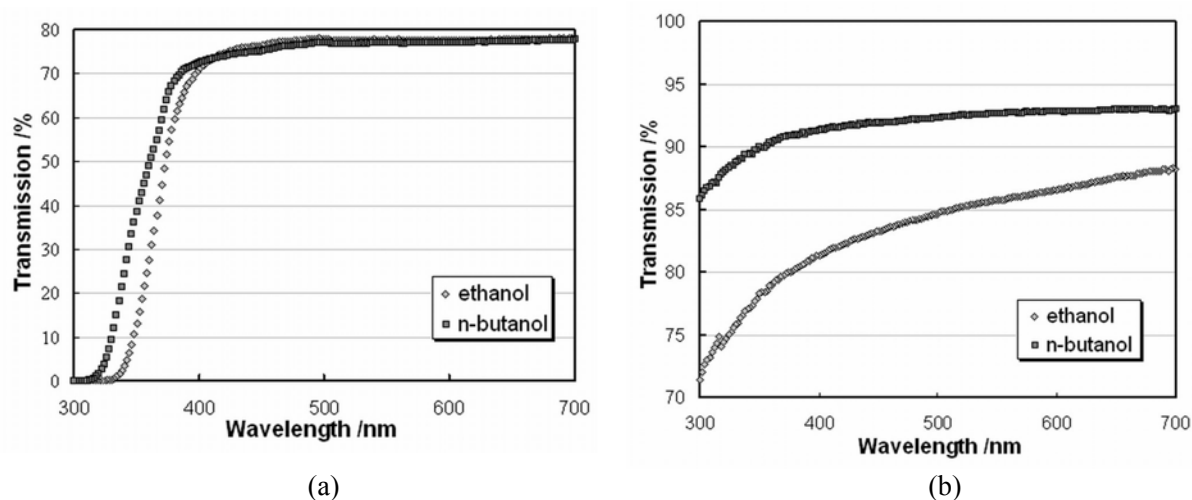


Figure 1. UV-VIS optical transmission of gels prepared using different solvents (a) and of corresponding sol-gel prepared films on quartz glass substrates (b).

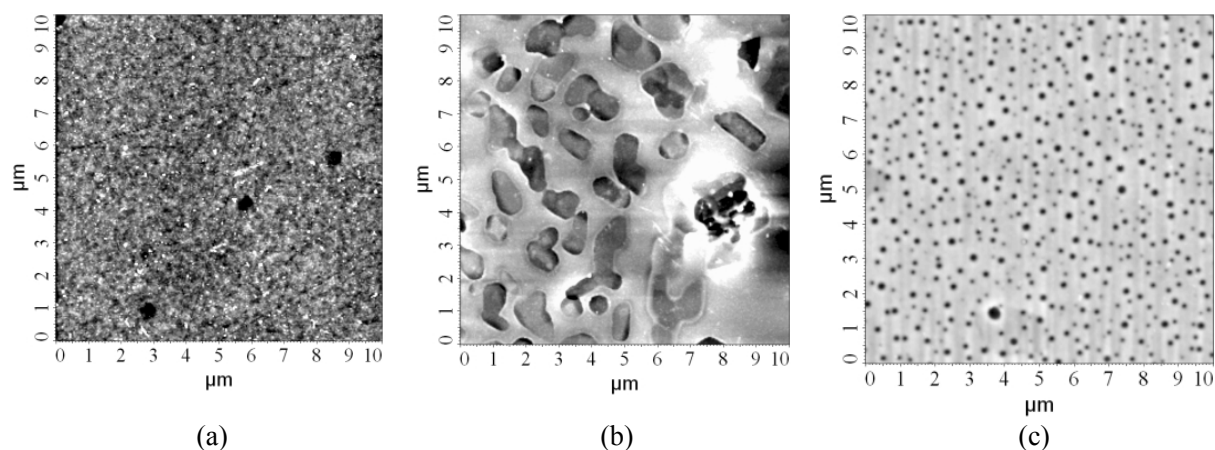


Figure 2. AFM-images of sol-gel layers:
(a) – 100 at% SnO₂; (b) – 10 at% SiO₂ – 90 at% SnO₂; (c) – 20 at% SiO₂ – 80 at% SnO₂.

The results of hydrogen gas sensitivity measurements at 200°C are summarized in table 1. The highest sensitivity was achieved by the sensor with 10 at% silica fraction possessing the highest porosity.

Table 1. Sensitivity (S) of tin oxide thin film sensors versus hydrogen concentration.

Composition	$S = \Delta R / R_{\text{air}}$			
	4500ppm	7500ppm	10500ppm	15000ppm
100 at% SnO ₂	0,38	0,42	0,45	0,48
10 at% SiO ₂ -90 at% SnO ₂	0,85	0,87	0,9	0,93
20 at% SiO ₂ -80 at% SnO ₂	0,76	0,79	0,83	0,86

Figure 3(a) shows the response curve of the corresponding sensor and figure 3(b) the response time in dependence on hydrogen concentration and silica fraction. The response time exhibits the typical dependence on the gas concentration, i.e., an increase of the response time with decreasing of gas concentration [15, 16]. As in the case of hydrogen sensitivity, the 10 at%SiO₂-90 at%SnO₂ sample provides the best properties, i.e., the fastest time response.

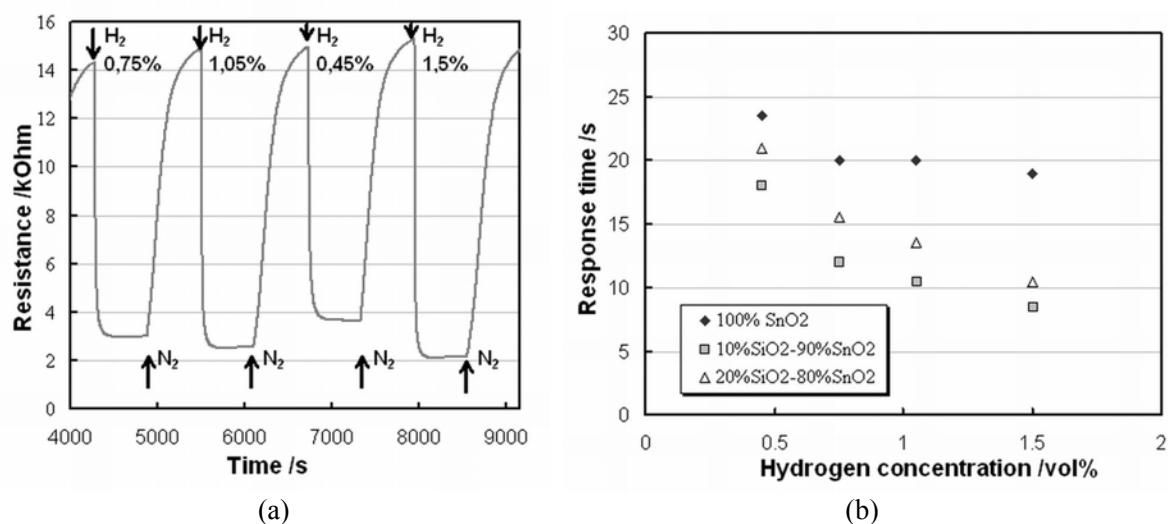


Figure 3. Response curve as obtained for the 20 at% SiO₂-80 at% SnO₂ sample (a) and dependence of response times on gas concentration (b) at a temperature of 200°C.

The hydrogen sensitivity of optimized sol-gel deposited films of this work ($S = 0.85-0.93$ cp. table 2) is sufficiently higher than that of commercial sol-gel fabricated gas sensors comprising Pt as catalyst ($S = 0.52$ at 200°C, 100 ppm H₂ [2], $S = 0.32$ at 200°C, 4000 ppm H₂ [17]). They exceed hydrogen sensitivity of thick films manufactured using pastes comprising nanometer sized grains of sol-gel fabricated tin oxide powders [18-20]. Comparable hydrogen sensitivity values were obtained in thin sol-gel films consisting of grains < 10 nm [21]. We attribute the somewhat higher hydrogen sensitivities (up to 0.98) reported for sol-gel films in [22-24] to an oxygen containing carrier gas (dry or synthetic air).

In order to test long-term stability of the hydrogen sensors fabricated in this work, seven hundred measuring cycles (cp. fig. 3) were carried out. No degradation of sensitivity was observed. Longer term investigations are in progress now.

4. Conclusions

Sol-gel deposition of oxide layers exhibiting advanced gas sensing properties requires an optimization of the porous film structure. In an optimized microstructure, nanopores provide high gas sensitivity due to an increased specific surface area and mesopores provide an efficient analyte transport decreasing sensor response and recovery times. SiO₂-SnO₂ nanocomposites comprising hierarchical macro-, meso- and micropores were fabricated using TEOS as a silicon source. TEOS is known to favour the formation of three-dimensional network of linked oxide particles in the gel leading to a proper pore structure in the annealed 10 at%SiO₂-90 at%SnO₂ composites.

Acknowledgements

This work was supported by contracts 16.740.11.0211, P399 and P2279 of the Federal Target Program “Scientific and Scientific-Pedagogical Personnel of Innovative Russia for the period 2009-2013”, and by the Erasmus Mundus External Co-operation Window Programme of the European Union (A.P.).

References

- [1] Seiyama T, Kato A, Fujiishi K and Nagatani M 1962 *Anal. Chem.* **34** 1502
- [2] Gong J, Fei W, Xia Z, Chen Q, Seal S and Chow L C 2003 *Proc. IEEE* **1** 124
- [3] Lu F, Liu Y, Dong M and Wang X 2000 *Sensors and Actuators B* **66** 225
- [4] Malyshev V V and Pislyakov A V 2008 *Sensors and Actuators B* **134** 913
- [5] Lee J-H 2009 *Sensors and Actuators B* **140** 319

- [6] Korotcenkov G 2005 *Sensors and Actuators B* **170** 209
- [7] Rouquerol J, Avnir D, Fairbridge C W, Everett D H, Haynes J M, Pernicone N, Ramsay J D F, Sing K S W and Unger K K 1994 *Pure & Appl. Chem.* **66** 1739
- [8] Delan A, Karuppasamy A and Schultheiß E 2009 *Plasma Processes and Polymers* **6** S731
- [9] Gu F, Wang S F, Lu M K, Cheng X F, Liu S W, Zhou G J, Xu D and Yuan D R 2004 *J. Cryst. Growth* **262** 182
- [10] Gaidi M, Hajjaji A, Smirani R, Bessais B and El Khakani M A 2010 *J. Appl. Phys.* **108** 063537
- [11] Maharolkar A P, Sudke Y, Kamble S and Tidar A 2010 *International Journal of Chemistry* **2** 250
- [12] Pires R M, Costa H F, Ferreira A G M and Fonseca I M A 2007 *J. Chem. Eng. Data* **52** 1240
- [13] Gracheva I E, Moshnikov V A, Karpova S S and Maraeva E V 2011 *J. Phys: Conf. Ser.* **291** 012017
- [14] Yang J, Hidajat K and Kawi S 2008 *Materials Letters* **62** 1441
- [15] Liewhiran C, Tamaekong N, Wisitsoraat A and Phanichphant S 2009 *Sensors* **9** 8996
- [16] Cukrov L M, McCormick P G, Galatsis K and Wlodarski W 2001 *Sensors and Actuators B* **77** 491
- [17] Gong J, Chen Q, Fei W, Seal S 2004 *Sensors and Actuators B* **102** 117
- [18] Wang Y-D, Ma C- L , Wu X-H, Sun X-D and Li H-D 2002 *Sensors and Actuators B* **85** 270
- [19] Pan Q, Xu J, Dong X and Zhang J 2000 *Sensors and Actuators B* **66** 237
- [20] Kim H-R, Choi K-I, Lee J-H and Akbar S A 2009 *Sensors and Actuators B* **136** 138
- [21] Hammond J W and Liu C-C 2001 *Sensors and Actuators B* **81** 25
- [22] Baik N S, Sakai G, Miura N and Yamazoe N 2000 *Sensors and Actuators B* **63** 74
- [23] Sakai G, Baik N S, Miura N and Yamazoe N 2001 *Sensors and Actuators B* **77** 116
- [24] Aroutiounian V 2007 *International Journal of Hydrogen Energy* **32** 1145